Chapter 62
Study of Atmospheric Neutrino Oscillation Parameters at the INO-ICAL Detector Using $\nu_e + N \rightarrow e + X$ Events

Aleena Chacko, D. Indumathi, James F. Libby, and Prafulla Kumar Behera

Abstract The India-based Neutrino Observatory will host a 50 kton magnetised tracking iron calorimeter with resistive plate chambers as its active detector element. We present the direction reconstruction of electron neutrino events with ICAL and the sensitivity of these events to neutrino oscillation parameters θ_{23} and δ_{CP}. We find that ICAL has adequate sensitivity to the CP violating phase δ_{CP}, with regions ranging $\delta_{CP} \sim 130$–$295°$ being excluded at 1σ for $\delta_{CP,\text{true}} = 0°$, from the sub-dominant electron neutrino oscillation channels. We also obtain a relative 1σ precision of 20% on the mixing parameter $\sin^2\theta_{23}$. We neither discuss the possible backgrounds to ν_e interaction in ICAL nor investigate the effect of systematic uncertainties.

62.1 Introduction

Neutrino experiments over the past few decades [1–7] have been successful in measuring most of the neutrino oscillation parameters, viz., neutrino mixing angle (θ_{12}, θ_{23}, θ_{13}), their mass squared differences (Δm^2_{12}, Δm^2_{32}) and CP violating phase (δ_{CP}), although their mass hierarchy is yet to be determined. One of the experiments of this kind is the India-based Neutrino Observatory (INO) which aims to study the atmospheric neutrinos to probe the mass hierarchy, independent of δ_{CP}. The pro-

A. Chacko (✉) · J. F. Libby · P. K. Behera
Indian Institute of Technology Madras, Chennai 600 036, India
e-mail: aleenachacko@physics.iitm.ac.in

J. F. Libby
e-mail: libby@iitm.ac.in

P. K. Behera
e-mail: behera@iitm.ac.in

D. Indumathi
The Institute of Mathematical Sciences, Chennai 600 113, India
e-mail: indu@imsc.res.in

Homi Bhabha National Institute, Training School Complex, Anushakti Nagar, Mumbai 400085, India

© Springer Nature Singapore Pte Ltd. 2021

P. K. Behera et al. (eds.), *XXIII DAE High Energy Physics Symposium*, Springer Proceedings in Physics 261,
https://doi.org/10.1007/978-981-33-4408-2_62

posed detector in INO is a magnetised iron calorimeter (ICAL) [8], built in three modules, with a resistive plate chamber (RPC) as its active detector element. The RPCs will be interleaved with iron layers (interaction medium) and pick-up strips are placed orthogonal to each other on either side of the RPC. ICAL is primarily optimised for muons.

The main signal of interest in ICAL will be charge current (CC) interactions of ν_μ (CCμ), but this paper focuses on the sub-dominant signal (nearly half of the ν_μ flux), namely the CC interactions of ν_e (CCe). These interactions are simulated for a 50 kton ICAL detector with 100-year exposure time by using the NUANCE [9] neutrino generator and incorporating the HONDA three-dimensional flux [10]. In Sects. 62.2 and 62.3, we study these NUANCE generated events. In Sects. 62.4 and 62.5, we describe the reconstruction of these events and their sensitivity to neutrino oscillation parameters θ_{23} and δ_{CP}.

62.2 Oscillation Probabilities

The neutrino oscillation probabilities of interest for CCe events are P_{ee} (electron survival probability) and $P_{\mu e}$ (muon disappearance probability) [11]. Figure 62.1 shows the effect of varying Δm^2_{32}, θ_{23} and δ_{CP}, for P_{ee} and $P_{\mu e}$. We see that the effect of varying Δm^2_{32} is opposite for P_{ee} and $P_{\mu e}$, which means the CCe events will provide very little sensitivity to Δm^2_{32}. Though not shown here, P_{ee} does not vary with different values of θ_{23} and δ_{CP}, but from Fig. 62.1 (bottom panel) $P_{\mu e}$ does. Therefore in this paper, we study only the ICAL sensitivity to $\sin^2\theta_{23}$ and δ_{CP} from CCe events.

62.3 Ultimate Sensitivity Study

We first examine in the regions of true neutrino energy (E_ν) and direction ($\cos\theta_\nu$) that have significant oscillation probabilities. We find that (Fig. 62.2), for $P_{ee} < 0.8$ and $P_{\mu e} > 0.1$ (to see significant oscillation signature), both probabilities have sensitivity in regions where $E_\nu > 2$ and $\cos\theta_\nu > 0$ (up-going neutrinos). The values for oscillation parameters are taken from [12]. Throughout this paper normal hierarchy is assumed.

Next, we use an ideal ICAL detector (100% efficiency and perfect resolution) to study the maximum sensitivity CCe events can provide to the oscillation parameters θ_{23} and δ_{CP}. We take a sample corresponding to 5 years of NUANCE generated events using unoscillated ν_e and ν_μ flux and incorporate oscillations on these events with the "accept-reject" method. From Fig. 62.3, we see the oscillation signatures in the same regions as in Fig. 62.2.

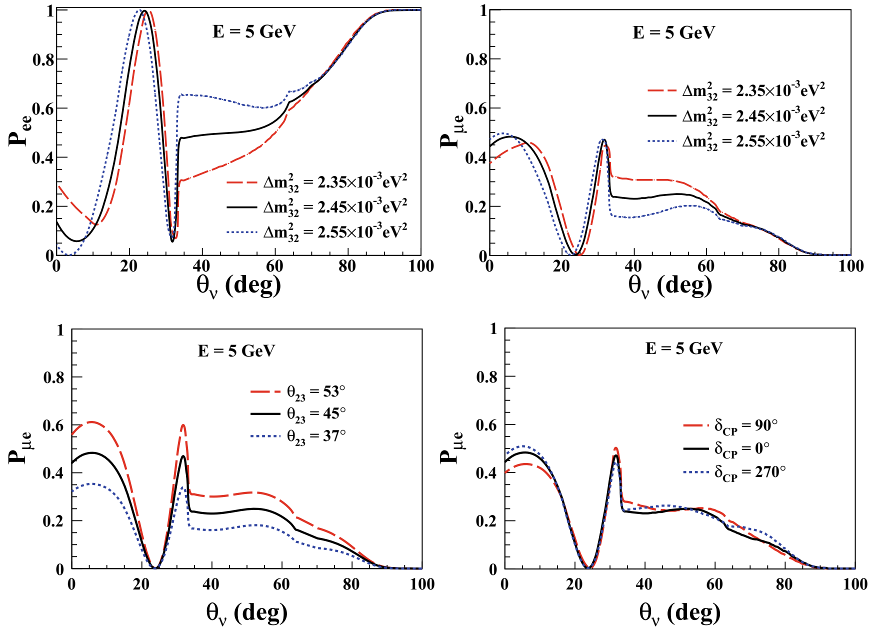

Fig. 62.1 P_{ee} and $P_{\mu e}$ (top panel) as a function of zenith angle, shown for three values of Δm^2_{32} ($2.55 \times 10^{-3}\mathrm{eV}^2$ [dotted blue line], $2.45 \times 10^{-3}\mathrm{eV}^2$ [solid black line] and $2.35 \times 10^{-3}\mathrm{eV}^2$ [dashed red line]). $P_{\mu e}$ (bottom panel) as a function of zenith angle, shown for three values of θ_{23} [left] (53° [dotted blue line], 45° [solid black line], 37° [dashed red line]) and three values of δ_{CP} [right] (270° [dotted blue line], 0° [solid black line] and 90° [dashed red line]), with $\theta_{13} = 8.33°$ and assuming the normal hierarchy

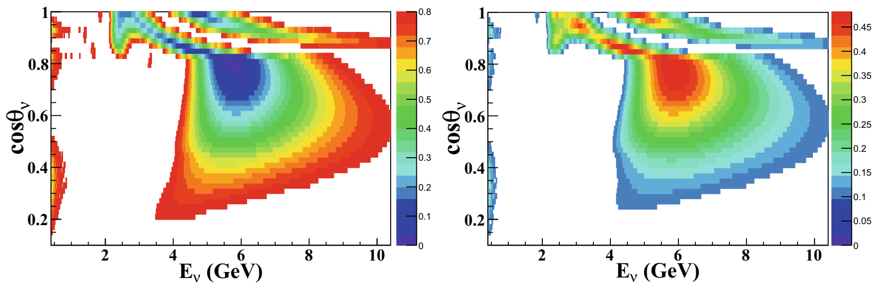

Fig. 62.2 $P_{ee} < 0.8$ (left) and $P_{\mu e} > 0.1$ (right) as a function of E_ν and $\cos\theta_\nu$

62.4 Reconstruction of CC*e* Events

To study the actual sensitivity that can be extracted from CC*e* events in ICAL, NUANCE generated unoscillated ν_e and ν_μ events are processed by a GEANT4 [13, 14] -based detector simulation of the ICAL detector. These simulated events have to be reconstructed to obtain E_ν and $\cos\theta_\nu$ from the final state particles (electrons and

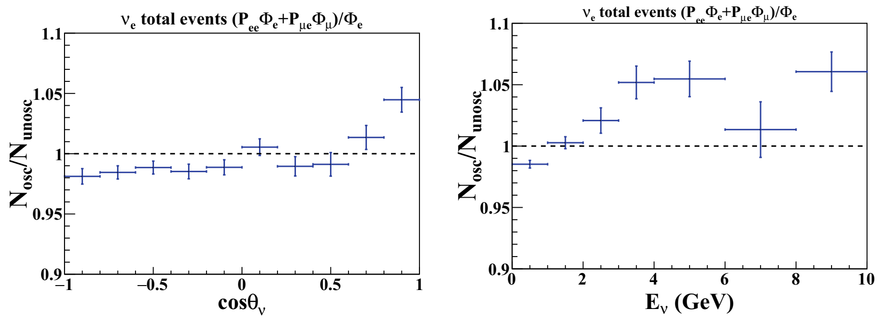

Fig. 62.3 Ratio of oscillated to unoscillated CCe events as a function of $\cos\theta_\nu$ (left) and E_ν (right), corresponding to 5 years of data

hadrons) in CCe interactions. Since electrons and hadrons only leave hits (shower) in the detector, unlike muons which leave a trail (track), an algorithm has to be developed to reconstruct the E_ν and $\cos\theta_\nu$ from the hit information.

62.4.1 *Direction Reconstruction*

The hit information in ICAL consist of the (x, y, z) positions and timing t of the hit. The x and y co-ordinates are the centres of the X- and Y-strips respectively, and the z co-ordinate is the centre of the RPC air-gap. We use the *raw-hit* method [15] which utilises this hit information to reconstruct the direction of the shower. In this method, the hit positions are plotted in two separate planes x-z and y-z, to avoid *ghost-hits* [15]. A straight line is fit to the hit positions in x-z and y-z planes, and from the slope of these fits $m_{x(y)}$, the average direction of the shower can be calculated as follows:

$$\theta = \tan^{-1}\left(\sqrt{m_x^2 + m_y^2}\right); \qquad \phi = \tan^{-1}\left(\frac{m_y}{m_x}\right). \tag{62.1}$$

The hits used for the reconstruction have to pass certain selection criteria. The timing window in which the hits are collected is restricted to 50 ns to ensure the hits are from the event under consideration. The hits have to be found in at least two layers and there must be a minimum of three hits in each event, to enable a straight line fit to hit positions. Around 54% of events are discarded due to this restriction. To pin the direction of the shower as up- or down-going, we make use of the slopes $m_{tx(ty)}$ of straight line fits to hit time in t_x-z(t_y-z) graphs. If m_{tx} and m_{ty} have opposite signs, those events are discarded and about 10% of the events are removed due to this restriction. The reconstruction efficiency ϵ_{reco} is defined as the percentage of reconstructed events (N_{reco}) in total CCe events (N) and relative directional efficiency ϵ_{dir}, is defined as percentage of correctly reconstructed events

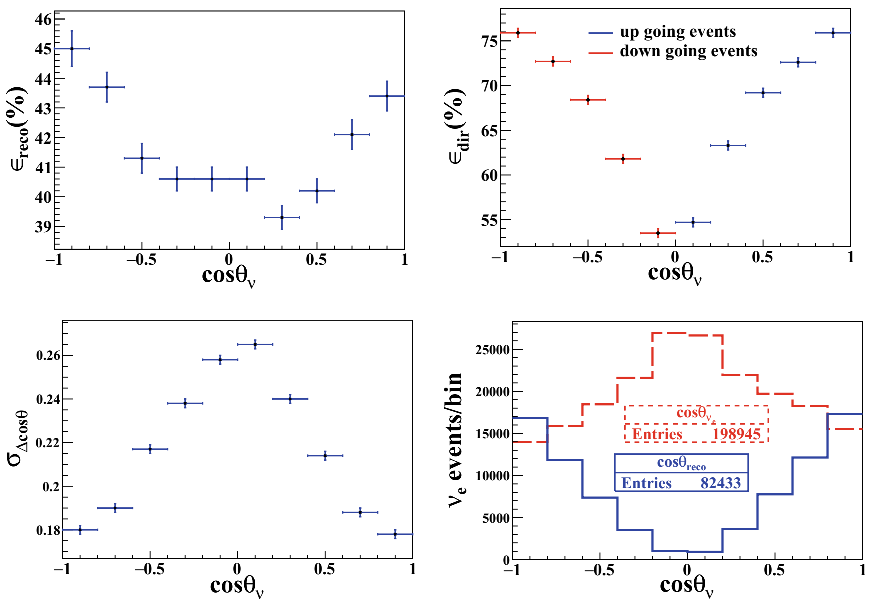

Fig. 62.4 Reconstruction efficiency, ϵ_{reco} (top left) and the relative directional efficiency ϵ_{dir} (top right) as a function of $\cos\theta_\nu$. $\cos\theta_\nu$ resolution (bottom left) and the distribution (bottom right) of the $\cos\theta_\nu$ (dashed red line) and reconstructed $\cos\theta_{reco}$ (solid blue line)

(N'_{reco}) as up- or down-going in total reconstructed events (N_{reco}) (62.2). The E_ν and $\cos\theta_\nu$ averaged values of ϵ_{reco} (Fig. 62.4, top left) and ϵ_{dir} (Fig. 62.4, top right) are $(41.7 \pm 0.2)\%$ and $(66.8 \pm 0.2)\%$, respectively, showing that we can distinguish an up-going event from a down-going event, which is crucial for the oscillation studies. The $\cos\theta_\nu$ resolution (Fig. 62.4, bottom left) improves for vertical events ($|\cos\theta_\nu > 0.5|$), as events traverse more layers in this direction. Figure 62.4 (bottom right) compares the $\cos\theta_\nu$ distribution before and after reconstruction.

$$\epsilon_{reco} = \frac{N_{reco}}{N}, \qquad \epsilon_{dir} = \frac{N'_{reco}}{N_{reco}}. \tag{62.2}$$

62.4.2 Energy Reconstruction

Unlike direction, E_ν cannot be reconstructed by directly using the hit information, rather we calibrate the total number of hits (n_{hits}) in an event to its E_ν. The calibration is done by grouping n_{hits} in different E_ν bins. The mean value of n_{hits} ($\overline{n}(E_\nu)$) in each of these distributions is plotted against the mean value $\overline{E}_\nu$ of the corresponding E_ν bin. This data is then fitted with

$$\bar{n}(E) = n_0 - n_1 \exp(-\bar{E}/E_0) \tag{62.3}$$

to obtain the values of constants n_0, n_1 and E_0 (Fig. 62.5[left]). Once we have the values of these constants, (62.3) is inverted to estimate reconstructed energy E_{reco} (Fig. 62.5[right]). The E_ν resolution improves with E_ν.

62.5 Oscillation Parameter Sensitivity

We perform a χ^2 analysis to assess the sensitivity of CCe events to oscillation parameters. We bin the 100-year "data" set (scaled down to 10 years for the fit) simulated with true oscillation parameters in the reconstructed observables of $\cos\theta_{\text{reco}}$ (ten bins of equal width) and E_{reco} (seven bins of unequal width in 0–10 GeV range). We define the Poissonian χ^2 as

$$\chi^2 = 2\sum_i \sum_j \left[(T_{ij} - D_{ij}) - D_{ij} \ln\left(\frac{T_{ij}}{D_{ij}}\right)\right], \tag{62.4}$$

where T_{ij} and D_{ij} are the "theoretically expected" and "observed number" of events respectively, in the ith $\cos\theta_{\text{reco}}$ bin and jth E_{reco} bin. Figure 62.6 shows $\Delta\chi^2$ as a function of $\sin^2\theta_{23}$ (left) and δ_{CP} (right), comparing binning in $\cos\theta_{\text{reco}}$, E_{reco} and in both. By binning in $\cos\theta_{\text{reco}}$ alone, we have a relative 1σ precision [8] of 20% on $\sin^2\theta_{23}$ and we are able to exclude $\delta_{CP} \sim 130$–$295°$ at 1σ for $\delta_{CP,true} = 0°$.

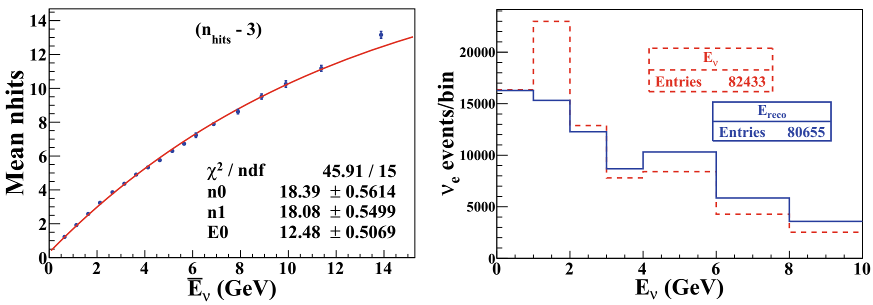

Fig. 62.5 Left: $\overline{n}(E)$ versus $\overline{E}_\nu$ and Right: the distribution of true E_ν (dashed red lines) and reconstructed E_{reco} (solid blue lines)

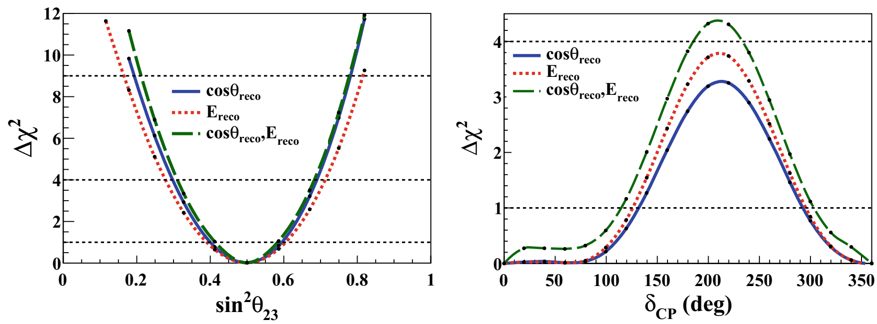

Fig. 62.6 $\Delta\chi^2$ as a function of $\sin^2\theta_{23}$ (left) and δ_{CP} (right) with bins in $\cos\theta_{\text{reco}}$ (solid blue lines) alone, E_{reco} (dotted red lines) alone and in both (dashed green lines) $\cos\theta_{\text{reco}}$ and E_{reco}. "Data" were generated with true $\sin^2\theta_{23} = 0.5$ and $\delta_{CP} = 0°$

62.6 Conclusion

In this paper, we have presented the reconstruction and oscillation parameter sensitivity of a pure sample of CCe events in ICAL. In reality, there are other types of events, like the neutral current events from both ν_μ and ν_e, which can be easily mis-identified as CCe events in ICAL. A significant fraction of CCμ events for which a track could not be reconstructed also mimics CCe hit patterns in ICAL. Hence, the next step would be finding selection criteria to separate CCe events from other types and analysing oscillation parameter sensitivity after including the mis-identified events. With CCe events alone, we find that ICAL has sufficient sensitivity to both oscillation parameters.

References

1. A. Gando et al., Phys. Rev. D **88**, 033001 (2013)
2. Daya Bay Collaboration, F. An et al., Phys. Rev. D **95** (2017)
3. Double Chooz Collaboration, Y. Abe et al., JHEP **1601** (2016)
4. RENO Collaboration, J.H. Choi et al., Phys. Rev. Lett. **116** (2016)
5. The KM3NeT collaboration, Adrián-Martínez et al., J. High Energ. Phys. **2017** (2017)
6. IceCube Collaboration, M.G. Aartsen et al., Phys. Rev. Lett. **120** (2018)
7. DUNE Collaboration, B. Abi et al., arXiv:1807.10334
8. ICAL Collaboration, S. Ahmed et al., Pramana **88**(5), 79 (2017)
9. D. Casper, Nucl. Phys. Proc. Suppl. **112**, 161 (2002)
10. M. Honda, T. Kajita, K. Kasahara, S. Midorikawa, Phys. Rev. D **83**, 123001 (2011)
11. D. Indumathi, M.V.N. Murthy, G. Rajasekaran, N. Sinha, Phys. Rev. D **74**, 053004 (2006)
12. C. Patrignani et al., Chin. Phys. C, **40**, 100001 (2016) and 2017 update
13. GEANT4 collaboration, S. Agostinelli et al., Nucl. Instrum. Meth. A **506**, 250 (2003)
14. J. Allison, K. Amako, J. Apostolakis, H. Araujo, P. Dubois et al., IEEE Trans. Nucl. Sci. **53**, 270 (2006)
15. M.M. Devi et al., JINST **13** (2018)